Preprints of the 21st IFAC World Congress (Virtual)
Berlin, Germany, July 12-17, 2020

Scheduling Parameter Reduction of Diesel Engine Air Path LPV Model by PCA and Autoencoder-Based Method

Mitsuo Hirata * **Teruhiko Asahi** * **Tatsuya Shiraishi** *
Masayasu Suzuki *

* *Utsunomiya University,*
7-1-2 Yoto, Utsunomiya, Tochigi 321–8585 Japan

Abstract: This study presents a method to reduce the number of scheduling variables in a linear parameter-varying (LPV) model of a diesel engine air path system. The reduction of these scheduling variables is very important because it exponentially decreases the computational complexity for the gain-scheduled LPV controller synthesis. Principal component analysis (PCA) and autoencoder (AE) based neural networks are applied to the LPV diesel engine's air path model, and the relationship between the accuracy of the reproduced scheduling variables and the number of the reduced scheduling parameters is evaluated via conduction of numerical simulations.

Keywords: Diesel engine, air path system, LPV model, autoencoder neural networks, principal component analysis, gain-scheduled control

1. INTRODUCTION

Modern diesel engines are typically equipped with variable geometry turbochargers (VGT) and an exhaust gas recirculation (EGR) system to meet the lower NOx, particulate matter (PM) emission, and higher thermal efficiency requirements (Xie et al., 2013; Stefanopoulou et al., 2000; Abd-Alla, 2002). However, these technologies increase the complexity of the system architecture and make it difficult to design the control system. In commercial vehicles, conventional controllers employ lookup tables that are optimized from the results of various experiments. However, the effort involved in constructing these tables has considerably increased because of the complexity of recent engines. Therefore, model-based controller design approaches are required as an alternative to traditional controller design methods.

The plant model of the diesel engines is highly nonlinear, and the controller gains have to be scheduled along with the operational conditions. For this control problem, a gain-scheduled H_∞ control (GS control) method can be a promising approach because it can cope with the plant nonlinearity, while also taking into account the plant uncertainties. In GS control, the plant model has to be represented by a linear parameter-varying (LPV) system. In most previous studies, the number of scheduling variables is restricted to one or two, because the number of the linear matrix inequalities (LMIs) to be solved for the GS control grows exponentially with the number of scheduling variables, and this produces a conservative result. However, in the LPV model of the diesel engine, many scheduling variables appear. Conventionally, the ad hoc reduction of the scheduling variables can be employed (Jung and Glover, 2006; Xiukun Wei and del Re, 2006; Liu et al., 2007; Lihua Liu et al., 2008); however, this compromises on the model accuracy, while making the synthesis problem tractable.

For the reduction of the scheduling variables, several approaches have been proposed. One such approach is a procedure based on principal component analysis (PCA) proposed by Kwiatkowski and Werner (2008). The ability of the PCA to reduce the data dimension makes it possible to reduce the number of scheduling variables in the LPV models. However, the PCA cannot capture the nonlinear nature of the scheduling variables, and a method based on the autoencoder (AE) neural networks was proposed by Rizvi et al. (2018). Unlike the PCA, the AEs can capture the nonlinear nature of the scheduling variables by employing the nonlinear activation function. In this study, we apply the PCA-based and AE-based reduction methods on the scheduling variables for the LPV model of the diesel engine air path system, and the relationship between the accuracy of the reduced model and the number of scheduling variables is evaluated via conduction of numerical simulations.

2. LPV MODEL REDUCTION

2.1 Problem formulation

An LPV state-space (LPV-SS) model is defined as follows:

$$\begin{aligned} \dot{x}_t &= A(\theta_t)x_t + B(\theta_t)u_t \\ y_t &= C(\theta_t)x_t + D(\theta_t)u_t \end{aligned} \tag{1}$$

where $x_t \in \mathcal{R}^{n_x}$, $u_t \in \mathcal{R}^{n_u}$, and $y_t \in \mathcal{R}^{n_y}$ represent the state vector, control input, and output at time t, respectively. The LPV-SS matrices $A(\theta_t)$, $B(\theta_t)$, $C(\theta_t)$ and $D(\theta_t)$ are assumed to be affine functions of θ_t as:

$$Q(\theta_t) = Q_0 + \sum_{i=1}^{l} \theta_{t,i} Q_i, \quad Q_i \in \mathcal{R}^{(n_x+n_y)\times(n_x+n_u)} \tag{2}$$

where

$$Q(\theta_t) = \begin{bmatrix} A(\theta_t) & B(\theta_t) \\ C(\theta_t) & D(\theta_t) \end{bmatrix} \in \mathcal{R}^{(n_x+n_y)\times(n_x+n_u)}. \quad (3)$$

The scheduling variables $\theta_t \in \mathcal{R}^l$ are a continuous function of the measurable signal $\mu_t \in \mathcal{R}^s$ as:

$$\theta_t = p(\mu_t), \quad p : \mathcal{R}^s \to \mathcal{R}^l. \quad (4)$$

For the given system Eq. (1), the problem of LPV model reduction can be defined as follows: find a mapping

$$\rho_t = q(\theta_t) = q(p(\mu_t)), \quad q : \mathcal{R}^l \to \mathcal{R}^m, \quad (5)$$

where $m < l$, such that the system matrices in

$$\begin{aligned} \dot{x}_t &= \hat{A}(\rho_t)x_t + \hat{B}(\rho_t)u_t, \\ y_t &= \hat{C}(\rho_t)x_t + \hat{D}(\rho_t)u_t \end{aligned} \quad (6)$$

have an affine dependence on ρ_t, and the LPV-SS of Eq. (6) approximates that of Eq. (1) sufficiently well.

2.2 PCA-based method

Let us assume that the scheduling variable θ_t have been sampled at the time instants $t = jT_s, j = 0, 1, \ldots, N-1$; thus, the following matrix is defined as:

$$\Theta = [\, \theta(0) \;\cdots\; \theta((N-1)T_s) \,] \in \mathcal{R}^{l\times N}. \quad (7)$$

The rows Θ_i of the data matrix need to be normalized by an affine map $\mathcal{N}_i$ to achieve scaled, zero mean data

$$\Theta_i^n = \mathcal{N}_i(\Theta_i), \quad \Theta_i = \mathcal{N}_i^{-1}(\Theta_i^n) \quad (8)$$

and a normalized data matrix

$$\begin{aligned} \Theta^n &= [\, \theta^n(0) \;\cdots\; \theta^n((N-1)T_s) \,] \in \mathcal{R}^{l\times N} \\ &= \mathcal{N}(\Theta) \end{aligned} \quad (9)$$

is defined.

In order to apply the PCA to the normalized data, a singular value decomposition is introduced as follows:

$$\Theta^n = [U_s, U_n] \begin{bmatrix} \Sigma_s & [0, \;\; 0] \\ 0 & [\Sigma_n, \; 0] \end{bmatrix} \begin{bmatrix} V_s^T \\ V_n^T \end{bmatrix} \quad (10)$$

where Σ_s has m significant singular values, and Σ_n has $l - m$ less significant singular values. Therefore, the following approximation holds

$$\begin{aligned} \hat{\Theta}^n &= [\, \hat{\theta}^n(0) \;\cdots\; \hat{\theta}^n((N-1)T_s) \,] \in \mathcal{R}^{l\times N} \\ &= U_s\Sigma_s V_s^T \\ &\simeq \Theta_n. \end{aligned} \quad (11)$$

The matrix $U_s \in \mathcal{R}^{l\times m}$ represents the basis of the significant column space of the data matrix Θ^n, and can be used to obtain a reduced mapping q from θ_t to ρ_t by computing

$$\rho_t = U_s^T \mathcal{N}(\theta_t). \quad (12)$$

The matrix

$$\hat{Q}(\theta_t) = \begin{bmatrix} \hat{A}(\rho_t) & \hat{B}(\rho_t) \\ \hat{C}(\rho_t) & \hat{D}(\rho_t) \end{bmatrix} \in \mathcal{R}^{(n_x+n_y)\times(n_x+n_u)} \quad (13)$$

in Eq. (6) can be calculated by substituting

$$\theta_t = \mathcal{N}^{-1}(U_s\rho_t) \quad (14)$$

into Eq. (3). Note that $\mathcal{N}^{-1}$ denotes the row-wise rescaling map.

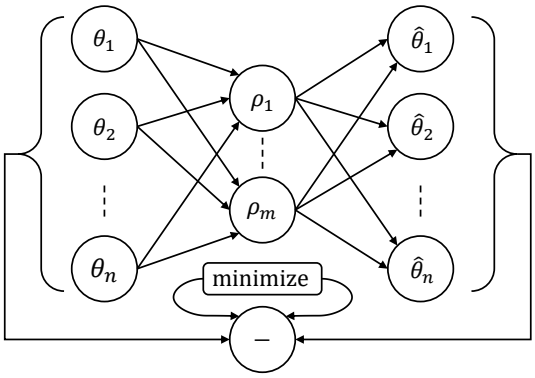

Fig. 1. Structure of autoencoder (two-layer).

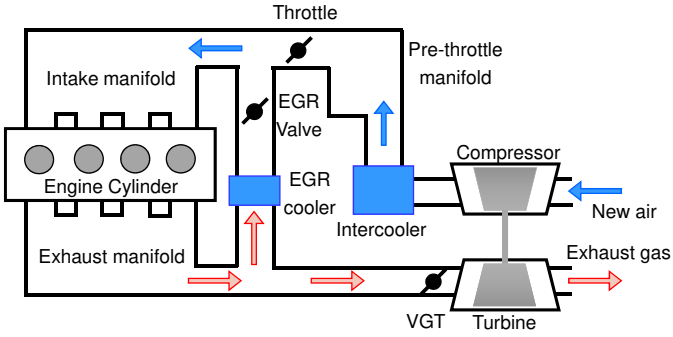

Fig. 2. Diesel engine air path system

2.3 Autoencoder neural network-based method

An autoencoder is a special neural network that is defined and trained to replicate its input at the output. The autoencoder has two parts: an encoder and a decoder, and each can have multiple layers. Fig. 1 is a simple autoencoder equipped with a single encoder layer and a single decoder layer. The weighting and bias parameters are optimized by minimizing the error between θ_t^n and $\hat{\theta}_t^n$. The nonlinear activation functions can be used for both of the encoder and decoder layers to obtain a reasonable low dimensional transformation of the scheduling variables. The nonlinear mapping obtained between θ_t^n and $\hat{\theta}_t^n$ for the reduced scheduling variables leads to solving of the other optimization problem to obtain a reduced LPV model for controller design (Rizvi et al., 2018).

3. DIESEL ENGINE AIR PATH SYSTEM

3.1 Plant model

The plant to be controlled is a direct-injection diesel engine manufactured by Toyota. It has four cylinders with a 2.8-L displacement. As shown in Fig. 2, the engine has a variable-geometry turbocharger (VGT) and an exhaust-gas recirculation (EGR) system.

The control inputs are the VGT valve closing u_{vgt} [% closed] and EGR valve opening u_{egr} [% open]; in addition, the controlled variables are the intake manifold pressure p_{im} [kPa] and EGR ratio $r_{egr} \in [0, 1]$ which is defined as

$$r_{egr} = \frac{W_{egr}}{W_{egr} + W_{pt}} \quad (15)$$

Table 1. List of variables

Symbol	Description	Units
W_c	Compressor mass flow	[kg/s]
W_{pt}	Pre-Throttle mass flow	[kg/s]
W_{egr}	EGR mass flow	[kg/s]
W_{ei}	Cylinder mass flow	[kg/s]
W_t	Turbine mass flow	[kg/s]
W_f	Fuel mass flow	[kg/s]
p_{pt}	Pre-throttle manifold pressure	[kPa]
p_{im}	Intake manifold pressure	[kPa]
p_{em}	Exhaust manifold pressure	[kPa]
P_c	Compressor power	[W]
P_t	Turbine power	[W]
T_{em}	Exhaust manifold temperature	[K]
T_{eo}	Cylinder out temperature	[K]
A_{pt}	Effective opening area (Pre-throttle)	[m^2]
A_{egr}	Effective opening area(EGR)	[m^2]
A_{vgt}	Effective opening area(VGT)	[m^2]
r_{egr}	EGR ratio	[%]
η_{tc}	Turbocharger efficiency	
ω_e	Engine speed	[rpm]
Q_f	Fuel injection quantity	[mm^3/st]

where W_{egr} [kg/s] and W_{pt} [kg/s] denote the EGR flow and throttle flow, respectively. Furthermore, we define the engine speed as ω_e [rpm]. The variables and constants used in the model are listed in Table 1 and Table 2. For simplicity, we assume that c_p, the specific heat at a constant pressure, and c_v, the specific heat at a constant volume, are constants, and all the gases considered in this research obey the ideal gas law.

The diesel engine air path model can be described by the following four differential equations (Hirata et al., 2018a,b).

$$\dot{p}_{im} = \frac{\gamma R}{V_{im}}(T_{pt}W_{pt} + T_{egr}W_{egr} - T_{im}W_{ei}), \tag{16}$$

$$\dot{p}_{em} = \frac{\gamma R}{V_{em}}(T_{eo}W_{ei} + T_{eo}W_f - T_{em}W_{egr} - T_{em}W_t), \tag{17}$$

$$\dot{p}_{pt} = \frac{\gamma R}{V_{pt}}(T_{ic}W_c - T_{pt}W_{pt}), \tag{18}$$

$$\dot{P}_c = \frac{1}{\tau_c}(\eta_{tc}P_t - P_c) \tag{19}$$

where

$$W_{ei} = \frac{\omega_e V_d \eta_v}{120RT_{im}}p_{im},$$

$$W_{pt} = A_{pt}\frac{p_{pt}}{\sqrt{RT_{pt}}}\psi\left(\frac{p_{im}}{p_{pt}}\right),$$

$$W_{egr} = A_{egr}\frac{p_{em}}{\sqrt{RT_{em}}}\psi\left(\frac{p_{im}}{p_{em}}\right),$$

$$W_t = A_{vgt}\frac{p_{em}}{\sqrt{RT_{em}}}\psi\left(\frac{p_{cab}}{p_{em}}\right),$$

$$W_c = \frac{P_c}{c_pT_{cab}\left[\left(\frac{p_{pt}}{p_{cab}}\right)^{\frac{\gamma-1}{\gamma}} - 1\right]},$$

Table 2. List of constants

Symbol	Description	Units
p_{cab}	Ambient pressure	[Pa]
T_{pt}	Pre-throttle manifold temperature	[K]
T_{im}	Intake manifold temperature	[K]
T_{cab}	Ambient temperature	[K]
T_{ic}	Intercooler out temperature	[K]
T_{egr}	EGR cooler out temperature	[K]
η_v	Cylinder efficiency	
R	Specific gas constant	[J/kg/K]
c_p	Specific heat at constant pressure	[J/kg/K]
γ	Ratio of specific values	
V_{im}	Volume (Intake manifold)	[m^3]
V_{em}	Volume (Exhaust manifold)	[m^3]
V_{pt}	Volume (Pre-throttle manifold)	[m^3]
V_d	Volume (Cylinder)	[m^3]
τ_c	Time constant (Compressor)	[s]
ρ_f	Fuel density	[kg/mm^3]
N_{cyl}	Number of cylinder	

$$P_t = W_t c_p T_{em}\left[1 - \left(\frac{p_{cab}}{p_{em}}\right)^{\frac{\gamma-1}{\gamma}}\right],$$

$$W_f = \rho_f Q_f \frac{N_{cyl}}{2}\cdot\frac{\omega_e}{60}$$

In this model, $T_{em} = T_{eo}$ is assumed, and T_{eo} is calculated using a nonlinear function of a fuel injection quantity Q_f followed by a first-order lag filter (Hirata et al., 2018b).

3.2 LPV model representation

By defining the state vector x, control input u, and output y as $x = [p_{im}, p_{em}, p_{pt}, P_c]^T$, $u = [A_{vgt}, A_{egr}]^T$, $y = [p_{im}, r_{egr}]^T$, we have the following LPV model.

$$\dot{x} = A(\theta_t)x + B(\theta_t)u, \tag{20}$$

$$y = C(\theta_t)x + D(\theta_t)u \tag{21}$$

where

$$\theta_t = [\theta_1, \ldots, \theta_9],$$

$$A(\theta_t) = \begin{bmatrix} -\frac{\gamma V_d \eta_v}{120V_{im}}\theta_1 & 0 & \frac{\gamma}{V_{im}}\theta_2 & 0 \\ \frac{\gamma R}{120V_{em}}\theta_3 & 0 & 0 & 0 \\ 0 & 0 & -\frac{\gamma}{V_{pt}}\theta_2 & \frac{\gamma RT_{ic}}{V_{pt}C_pT_{cab}}\theta_4 \\ 0 & 0 & 0 & -\frac{1}{\tau_c} \end{bmatrix},$$

$$B(\theta_t) = \begin{bmatrix} 0 & \frac{\gamma RT_{egr}}{V_{im}}\theta_5 \\ -\frac{\gamma}{V_{em}}\theta_6 & -\frac{\gamma}{V_{em}}\theta_7 \\ 0 & 0 \\ \frac{\eta_{tc}c_p}{\tau_c}\theta_8 & 0 \end{bmatrix},$$

$$C(\theta_t) = \begin{bmatrix} 10^{-3} & 0 & 0 & 0 \\ 0 & \theta_9 & 0 & 0 \end{bmatrix}, \quad D(\theta_t) = 0.$$

The elements of the scheduling variables θ_t are described as follows:

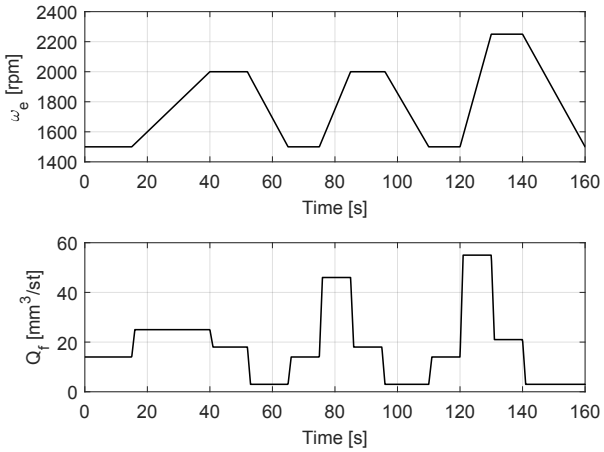

Fig. 3. Simulation pattern (engine speed ω_e and fuel injection quantity Q_f).

$$\theta_1 = \omega_e,$$

$$\theta_2 = A_{pt}\sqrt{RT_{pt}}\psi\left(\frac{p_{im}}{p_{pt}}\right),$$

$$\theta_3 = T_{em}\omega_e\left(\frac{V_d\eta_v}{RT_{im}} + \frac{\rho_f Q_f N_{cyl}}{p_{im}}\right),$$

$$\theta_4 = \frac{1}{\left[\left(\frac{p_{pt}}{p_{cab}}\right)^{\frac{\gamma-1}{\gamma}} - 1\right]},$$

$$\theta_5 = \frac{\psi\left(\frac{p_{im}}{p_{em}}\right)p_{em}}{\sqrt{RT_{em}}},$$

$$\theta_6 = \sqrt{RT_{em}}p_{em}\psi\left(\frac{p_{cab}}{p_{em}}\right),$$

$$\theta_7 = \sqrt{RT_{em}}p_{em}\psi\left(\frac{p_{im}}{p_{em}}\right),$$

$$\theta_8 = p_{em}\sqrt{\frac{T_{em}}{R}}\psi\left(\frac{p_{cab}}{p_{em}}\right)\left[1 - \left(\frac{p_{cab}}{p_{em}}\right)^{\frac{\gamma-1}{\gamma}}\right]$$

$$\theta_9 = \frac{\frac{A_{egr}}{\sqrt{RT_{em}}}\psi\left(\frac{p_{im}}{p_{em}}\right)}{A_{egr}\frac{p_{em}}{\sqrt{RT_{em}}}\psi\left(\frac{p_{im}}{p_{em}}\right) + A_{pt}\frac{p_{pt}}{\sqrt{RT_{pt}}}\psi\left(\frac{p_{im}}{p_{pt}}\right)},$$

where

$$\psi\left(\frac{p_{out}}{p_{in}}\right) = \begin{cases} \frac{1}{\sqrt{2}}, & \left(0 \le \frac{p_{out}}{p_{in}} < 0.5\right) \\ \sqrt{2\frac{p_{out}}{p_{in}}\left(1 - \frac{p_{out}}{p_{in}}\right)}, & \left(0.5 \le \frac{p_{out}}{p_{in}} < 1\right) \end{cases}.$$

3.3 LPV model reduction by PCA-based method

Θ in Eq. (7) was obtained by performing the mode operation test in which the engine speed and fuel injection quantity were varied as shown in Fig. 3. Since the sampling period of simulation was 1 ms and the obtained data was comparatively longer, the data was re-sampled with the sampling period of 200 ms. The data length was reduced from 160001 to 801. Furthermore, it was normalized so as to have zero mean and unit variance, and Θ^n in Eq. (9) was obtained. The time responses of $\theta_i^n, i = 1, \ldots, 9$ are shown in Fig. 4.

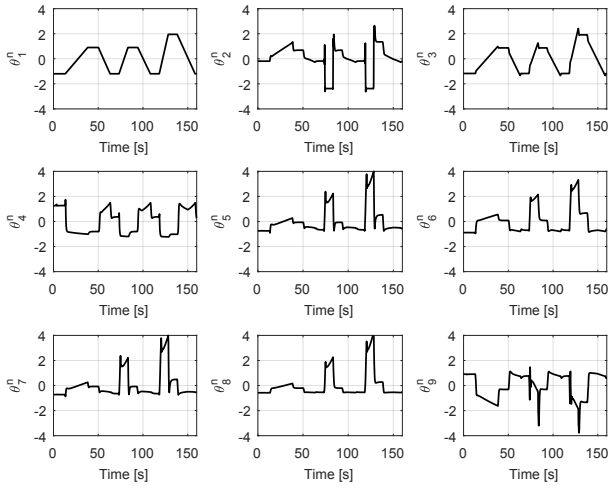

Fig. 4. Normalized scheduling variables θ_i^n.

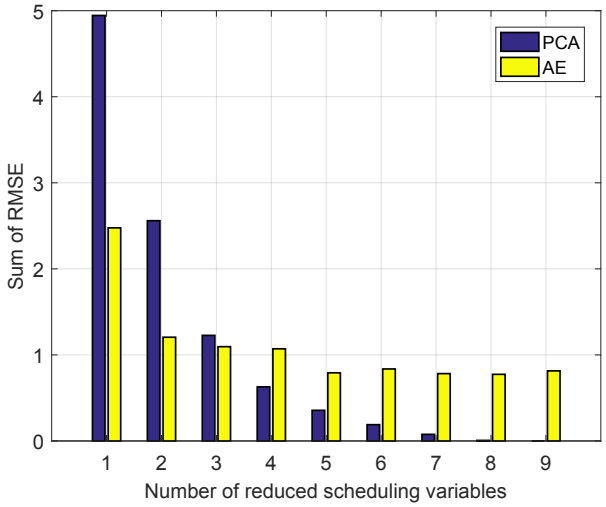

Fig. 5. Sum of RMSE of estimated θ^n for different number of scheduling variables.

Then, we applied the singular value decomposition Eq. (10) to Θ_n for $m = 1, 2, \ldots, 9$, and the estimated scheduling parameters $\hat{\Theta}_n$ in Eq. (11) were calculated. The sum of the RMSE

$$J = \sum_{i=1}^{l}\sqrt{\frac{(\theta_i^n - \hat{\theta}_i^n)^2}{N}}$$

was shown in Fig. 5. This RMSE was reduced by increasing the number of the reduced scheduling variables. For $m = 2$, the time responses of θ^n and $\hat{\theta}^n$ are shown in Fig. 6. From this figure, some estimation error is confirmed for θ_1^n, θ_4^n, and θ_9^n. These errors were reduced by increasing the number of the reduced scheduling variables to $m = 3$ as shown in Fig. 7. θ_4^n still reflects some error; however, other variables replicate the original scheduling variables well. This can be confirmed by Fig. 8 which indicates the RMSE of θ_i^n for $m = 1, 2, 3$.

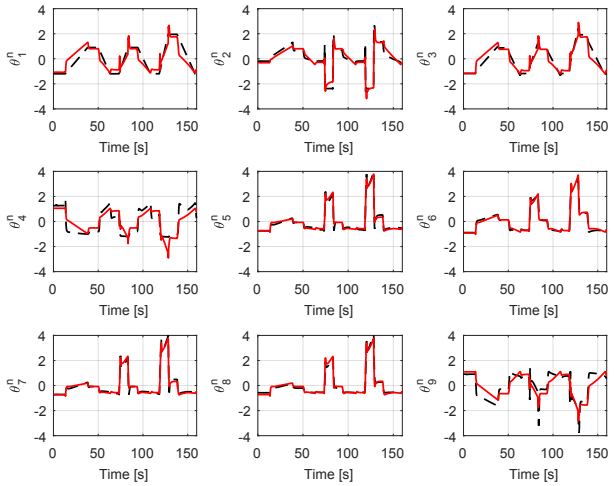

Fig. 6. Estimation result (m=2).

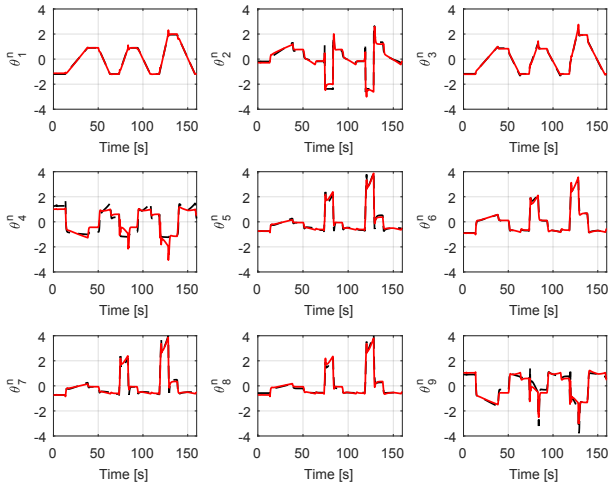

Fig. 7. Estimation result (m=3).

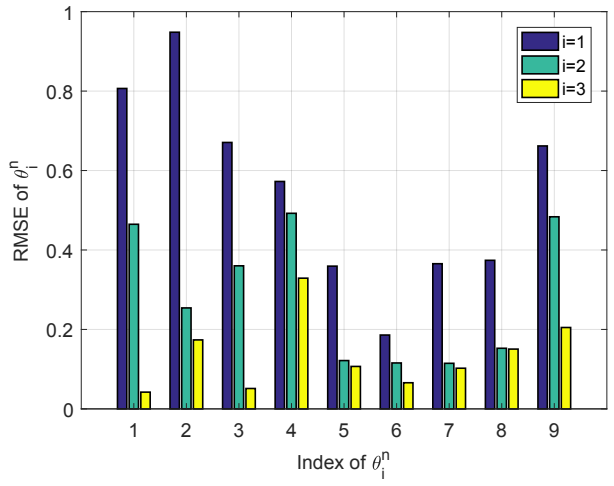

Fig. 8. Estimation error (m=1,2, and 3).

3.4 LPV model reduction by autoencoder-based method

We constructed an autoencoder to have four layers for both the encoder and decoder parts. A *selu* (scaled exponential linear unit) function was used as an activation function for the first three layers and a *linear* function was used for the last layer for both the encoder and decoder parts. The *selu* is defined as follows:

$$selu(x) = \begin{cases} \lambda x & (x > 0) \\ \lambda\alpha(e^x - 1) & (x \leq 0) \end{cases} \tag{22}$$

where α and λ are constants, and they are chosen such that the mean and variance of the inputs are preserved between the two consecutive layers (Klambauer et al., 2017). The structure of the autoencoder neural network is shown in Table 3. A Keras neural network API in the Tensorflow library that is written in Python was used to optimize the autoencoder.

The autoencoder was trained so as to minimize the mean squared reconstruction error of $\theta^n - \hat{\theta}^n$ for the normalized data Θ^n —the same data that was used for the PCA-

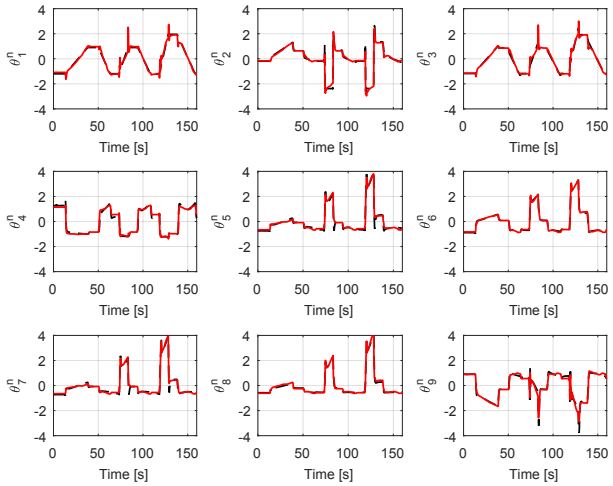

Fig. 9. Estimation result (m=2).

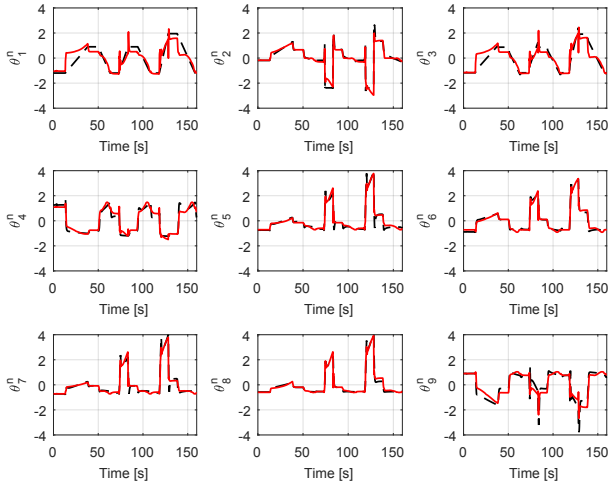

Fig. 10. Estimation result (m=1).

Table 3. Structure of autoencoder

Layer	Activation func.	size
Encoder-1	selu	9
Encoder-2	selu	7
Encoder-3	selu	5
Encoder-4	linear	m
Decoder-1	selu	5
Decoder-2	selu	7
Decoder-3	selu	9
Decoder-4	linear	9

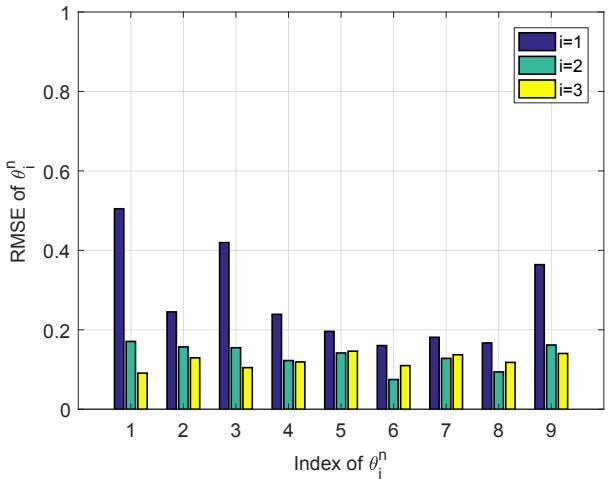

Fig. 11. Estimation error (m=1,2, and 3).

based method. An Adagrad optimizer was used to learn the neural network.

The time response of the reconstructed scheduling variables $\hat{\theta}^n$ is shown in Fig. 9 for $m = 2$. From this figure, we can confirm that all the reconstructed scheduling variables replicate the original ones, even though the number of the reduced scheduling variables is two. Fig. 10 shows the result when $m = 1$, and it can be seen that the performance is similar to the PCA-based method for $m = 2$. This can be confirmed by comparing Fig. 8 and Fig. 11 which indicate the RMSE of θ_i^n for $m = 1, 2, 3$.

4. SUMMARY

In this study, we applied two scheduling parameter reduction methods on the LPV model of a diesel engine air path system, and the accuracy of the reconstructed scheduling variables was evaluated. In the PCA-based method, a minimum of three scheduling variables were required to replicate θ^n. On the other hand, we confirmed through simulations that the AE-based method exhibits the potential to reduce the number of the scheduling variables by one, as compared to the PCA-based method. As a potential future work, a gain-scheduled H_∞ controller can be designed using the reduced LPV model, and the evaluation of the relationship between the control performance and the number of the reduced scheduling variables will be insightful.

ACKNOWLEDGEMENTS

A part of this work is the result of a collaborative research program with the Research association of Automotive Internal Combustion Engines (AICE) for fiscal year 2019. The authors gratefully acknowledge the concerned personnel.

REFERENCES

Abd-Alla, G. (2002). Using exhaust gas recirculation in internal combustion engines: a review. *Energy Conversion and Management*, 43(8), 1027–1042. doi: https://doi.org/10.1016/S0196-8904(01)00091-7.

Hirata, M., Hayashi, T., Koizumi, J., Takahashi, M., Yamasaki, Y., and Kaneko, S. (2018a). Modeling of diesel engine air path system using a discrete combustion model and two-degree-of-freedom control. In *Proc. of Symposium for Combustion Control*, 207–214.

Hirata, M., Hayashi, T., Koizumi, J., Takahashi, M., Yamasaki, Y., and Kaneko, S. (2018b). Two-degree-of-freedom H_∞ control of diesel engine air path system with nonlinear feedforward controller. In *Proc. of the 5th IFAC Conference on Engine and Powertrain Control, Simulation and Modeling*, 574–580.

Jung, M. and Glover, K. (2006). Calibratable linear parameter-varying control of a turbocharged diesel engine. *IEEE Transactions on Control Systems Technology*, 14(1), 45–62. doi:10.1109/TCST.2005.860513.

Klambauer, G., Unterthiner, T., Mayr, A., and Hochreiter, S. (2017). Self-normalizing neural networks.

Kwiatkowski, A. and Werner, H. (2008). PCA-based parameter set mappings for LPV models with fewer parameters and less overbounding. *IEEE Transactions on Control Systems Technology*, 16(4), 781–788. doi: 10.1109/TCST.2007.903094.

Lihua Liu, Xiukun Wei, and Tao Zhu (2008). Quasi-LPV gain scheduling control for the air path system of diesel engines. In *2008 Chinese Control and Decision Conference*, 4893–4898. doi:10.1109/CCDC.2008.4598258.

Liu, L., Wei, X., and Liu, X. (2007). LPV control for the air path system of diesel engines. In *2007 IEEE International Conference on Control and Automation*, 873–878. doi:10.1109/ICCA.2007.4376481.

Rizvi, S.Z., Abbasi, F., and Velni, J.M. (2018). Model reduction in linear parameter-varying models using autoencoder neural networks. In *2018 Annual American Control Conference (ACC)*, 6415–6420. doi: 10.23919/ACC.2018.8431912.

Stefanopoulou, A.G., Kolmanovsky, I., and Freudenberg, J.S. (2000). Control of variable geometry turbocharged diesel engines for reduced emissions. *IEEE Transactions on Control Systems Technology*, 8(4), 733–745. doi: 10.1109/87.852917.

Xie, H., Li, S., Song, K., and He, G. (2013). Model-based decoupling control of VGT and EGR with active disturbance rejection in diesel engines. *IFAC Proceedings Volumes*, 46(21), 282–288. doi: https://doi.org/10.3182/20130904-4-JP-2042.00149. 7th IFAC Symposium on Advances in Automotive Control.

Xiukun Wei and del Re, L. (2006). Modeling and control of the boost pressure for a diesel engine based on LPV techniques. In *2006 American Control Conference*. doi: 10.1109/ACC.2006.1656496.